PHYSICAL REVIEW B **82**, 201406(R) (2010)

Controlled surface functionalization via self-selective metal adsorption and pattern transformation on the vicinal Si(111) surface

A. L. Chin,[1] F. K. Men,[1,*] and Feng Liu[2]
[1]*Department of Physics, National Chung Cheng University, Chia-Yi 621 Taiwan, Republic of China*
[2]*Department of MSE, University of Utah, Salt Lake City, Utah 84112, USA*
(Received 3 November 2010; published 16 November 2010)

We demonstrate a self-selective metal adsorption and pattern transformation process on vicinal Si(111) surfaces. When Au atoms are deposited onto the self-organized periodic Si(111) surface patterns, the Au atoms self-select to adsorb predominantly onto one of the two distinct domains, the Si(111) terrace or the step-bunched facet at different Au coverage. This leads to a systematic transformation of the surface pattern, whose domain population changes while its periodicity remains intact with the increasing Au coverage. A stress-domain model is used to explain the observed phenomenon. Our findings suggest a unique method for controlled functionalization of surfaces at the nanoscale, as illustrated further by domain-selective self-assembly of uniform $CoSi_2$ nanoclusters on the Au-functionalized vicinal Si(111) surface.

DOI: 10.1103/PhysRevB.82.201406 PACS number(s): 68.35.−p, 68.37.Ef, 81.16.Rf

One fundamental phenomenon in surface science is the structural transition of a surface upon atomic and molecular adsorption, which has significant technological implications in functionalizing the surface for various applications, such as surface catalysis, patterning, and self-assembly of nanostructures. In general, surface structural transition is commonly manifested by an atomic surface reconstruction which depends on the coverage of adsorbates. For example, upon Au deposition, the (7×7) reconstructed Si(111) surface undergoes a series of transitions to form the (5×2) (Refs. 1 and 2) and $(\sqrt{3}\times\sqrt{3})$ (Refs. 3–5) superstructures with the increasing Au coverage. On a vicinal Si(111) surface, Au adsorption also induces transitions in surface step morphology and facets.[6,7] On the other hand, surface adsorption changes not only the surface energy but also the surface stress, which gives rise to another manifestation of structural transition in forming stress-domain patterns with long-range order as a special class of surface self-organization phenomena.[8–10]

In this Rapid Communication, we demonstrate a series of transitions on Au-deposited vicinal Si(111) surfaces, which exhibit a much richer behavior than what have been observed in either the surface reconstruction on the nominal surfaces[1–5] or faceting on the vicinal surfaces.[6,7] They reveal different physical insights, characterized by an intriguing correlation between the adsorption-induced atomic-scale structural reconstruction with the nanoscale morphological transformation of stress domains. We show that when Au atoms are deposited onto a vicinal Si(111) surface, which has self-organized into a nanoscale periodic pattern consisting of two distinct structural domains,[8–10] i.e., the terrace and the step-bunched facet, they self-select to adsorb predominately onto one of the two domains at a given Au coverage and simultaneously transform the Au-adsorbed domain structure. Most interestingly, while the relative population of the two domains changes with the Au coverage, the periodicity of the pattern remains constant, which are defined by the characteristic length scales of stress-domain patterns and geometric relations of facet and surface miscut angles. Our findings suggest an original technique for controlled functionalization of a surface at the nanometer scale. An example demonstrating selective self-assembly of $CoSi_2$ nanoclusters on the Au-functionalized Si(111) surface pattern is given.

Using scanning tunneling microscope (STM), we have investigated the structural and morphological changes upon Au deposition on vicinal Si(111) surfaces with miscut angles between 2° and 6° toward the $[\bar{2}11]$ direction. The surfaces were cleaned by degassing at 700 °C for several hours in a vacuum chamber (base pressure $<1\times10^{-10}$ mbar) followed by heating a few times to 1250 °C for ~10 s each. The cleaned surfaces were then annealed at 900 °C for a few minutes followed by slow cooling to room temperature at a rate of 1 °C/s.

The Au atom source was produced by heating an Au wire (99.99+% pure) placed in a Mo crucible to ~1000 °C via electron bombardment. The typical deposition rate was 1/300 monolayer [ML, 1 ML$=7.83\times10^{14}$ atoms/cm^2, the unreconstructed Si(111) surface-atom density] per second. The Si substrate temperature was maintained at 700 °C during Au deposition. After the Au deposition, the substrate was cooled down to room temperature at 1 °C/s. Cobalt atoms, produced by heating a 2 mm diameter Co rod (99.9% pure) via electron bombardment, were deposited at room temperature. Annealing of the Co-deposited surface was needed for the formation of nanoclusters. All observations were made at room temperature. The STM images, unless stated otherwise, are displayed in derivative mode to suppress the large height difference within a facet to give a better view of the facet configuration.

For a clean Si(111) vicinal surface with a miscut toward the $[\bar{2}11]$ direction, a periodic pattern of alternating facets and terraces has been observed with low-energy electron microscopy[8,9] and STM,[10] as shown in Fig. 1. The period of such stress-domain patterns was shown to be nearly constant of 66 nm, independent of surface miscut angle, while the facet width increases linearly with the miscut angle.[10] For a 6° miscut surface [Figs. 1(a) and 1(b)], the facet width is ~31 nm. The facet consists of disordered 1×1 narrow terraces with a width of ~2.8 nm separated by double bilayer height (0.62 nm) steps whereas the terrace displays the low-

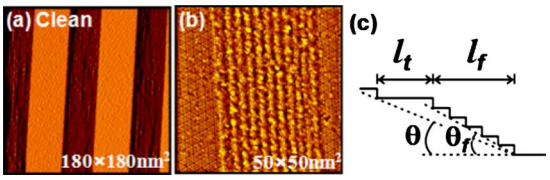

FIG. 1. (Color online) (a) STM image of a 6° miscut clean Si(111) surface. (b) Magnification of (a) showing the facet structure. (c) Schematics of stress-domain surface pattern.

energy (7×7) dimer-adatom-stacking-fault (DAS) reconstruction.[11]

It is well known that the periodic pattern of the clean vicinal surface consists of a stress-domain structure[12–14] and the constant periodicity independent of surface miscut originates from a two-stage self-organization process.[10] The equilibrium domain population reflects a relative balance between surface (facet) energies and elastic relaxation energies. The surface free energy per area of such stress domains can be expressed as[10]

$$F = F_f(l_f \sec\ \theta_f) + F_t(L - l_f) - \frac{c}{L}\ln\left[\frac{L}{\pi a}\sin\left(\frac{l_f}{L}\pi\right)\right] + \frac{2\gamma}{L}, \tag{1}$$

where $L=l_f+l_t$ is the periodicity, l_f and l_t are, respectively, the facet and terrace width and θ and θ_f are, respectively, the miscut and the facet angle, as shown in Fig. 1(c). F_f and F_t are, respectively, the surface energy per area of the facet and terrace. c is a constant related to the surface stress discontinuity at the facet-terrace boundary, γ is the boundary energy, and a is the effective boundary width, a cut-off length to avoid elastic divergence.

Figure 2 shows the evolution of surface morphology with the increasing Au coverage. At 0.07 ML of Au coverage, we observe the first change in the ordered surface domain structure: the stepped facet expands from ~31 to ~55 nm while the flat terrace shrinks from ~35 to ~11 nm [see Fig. 2(a)], as the mini (1×1) terraces within the facet transform into a much wider (5×5) DAS-like superstructure with a uniform width of 5.0 nm, 1.5 times of the (5×5) unit cell, as shown in Fig. 2(b). In a sharp contrast, the static structure of the

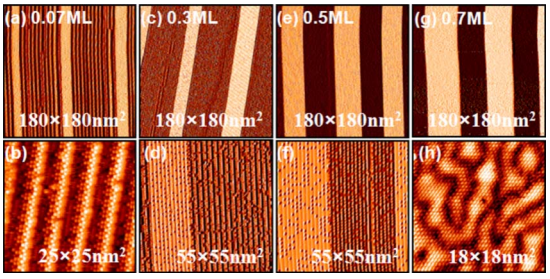

FIG. 2. (Color online) Surface morphology vs Au coverage. The Au coverage is labeled in each image pair, where the top (bottom) image is a large (small) area scan. Darker regions in each image have large height differences, representing the facets with the exception of Figs. 1(b) and 1(h), where raw data are displayed. Images were taken from 6°-miscut samples.

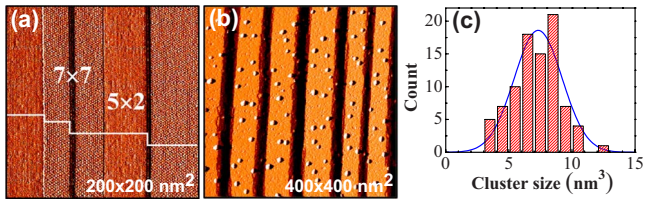

FIG. 3. (Color online) (a) Phase separation on a nominally flat Si(111) surface. Terraces and steps are marked. (b) Formation of $CoSi_2$ nanoclusters on terraces. Au was first deposited onto a 4° Si(111)-(7×7) surface such that the terraces and facets displayed, respectively, the (5×2) superstructure and 1.6 nm mini terraces, followed by depositing 0.2 ML of Co. (c) Cluster size distribution. The average cluster size is 7.1±1.9 nm. The blue Gaussian curve is to guide the eyes.

reduced (7×7) terraces [Fig. 1(a)] is unaffected by the Au deposition, although some mobile Au atoms may exist but cannot be resolved by STM. This indicates a high selectivity in Au surface adsorption, as the Au atoms adsorb predominately onto one of the two domains in the surface pattern, i.e., the facet, signifying a large disparity in Au reactivity with the facet versus the terrace. The selective Au adsorption transforms the facet structure by expanding the mini terrace width between the steps while keeping the step height unchanged, as shown in Fig. 2(b). This in turn transforms the surface morphology, as the stepped facet domain grows in width at the expense of the (7×7) terrace domain, but the periodicity of the domain pattern remains intact, as shown in Fig. 2(a).

To examine the reactivity of a (7×7) terrace with Au atoms, we have performed a separate "benchmark" experiment by purposely depositing less than 0.5 ML (0.1 ML) of Au onto a nominally flat (7×7) surface, as shown in Fig. 3(a). Interestingly, we found that some terraces would convert into patches of (5×2) superstructures while others remained unchanged. A (5×2) superstructure has a coverage of ~0.5 ML of Au,[2,15] which means Au atoms must have segregated from the surrounding (7×7) terraces to make up the needed local high Au density. Our measured ratio of the (5×2) over the (7×7) areas is consistent with the amount of deposited Au atoms. Thus, instead of forming one surface phase of nominal Au coverage, the surface phase separate into two domains: one with ~0.5 ML Au coverage and the other with no (or very low) Au coverage. This demonstrates that a perfect (7×7) terrace has the tendency to either stay free of Au atoms or transform directly to (5×2) structure with high Au coverage (except possible small amount of mobile Au atoms), if the "local" Au coverage is lower than what is needed for forming the (5×2) superstructure. This explains why the initially deposited Au atoms self-select to adsorb predominantly onto the facet domains, as shown in Figs. 2(a) and 2(b), because the facets are far more reactive than the clean (7×7) terraces with a very low coverage of Au.

At 0.3 ML, we observe the second change in the surface domain structure: the facet shrinks slightly from ~55 to ~48 nm while the flat terrace expands from ~11 to ~18 nm [see Fig. 2(c) vs Fig. 2(a)], as the width of the mini

terraces within the facet reduces to 2.2 nm [see Fig. 2(d) vs Fig. 2(b)] and the flat terraces transform from the (7×7) reconstruction to the (5×2) superstructure [Fig. 2(d)]. The (5×2) superstructure observed here is identical to that observed on a nominally flat Au-covered Si(111) surface.[1] It clearly indicates that this time Au atoms have selectively adsorbed onto the terrace domains because the (5×2) structure is known to have a ~0.5 ML coverage of Au. We note that the periodicity of the surface pattern remains preserved, as shown in Fig. 2(c).

At 0.5 ML, we observe the third transition in the surface domain structure: the facet shrinks from ~48 to ~35 nm while the terrace expands from 18 to 31 nm [see Fig. 2(e) vs Fig. 2(c)], as the facet structure changes by a reduced step-step separation from 2.2 nm [Fig. 2(d)] to 1.6 nm [Fig. 2(f)] while the terrace retains the (5×2) superstructure. So, once again we see a self-selective adsorption of Au atoms onto the facets in this range of Au coverage. Furthermore, the overall periodicity remains unchanged as the terraces grow in width at the expense of the facets. Lastly, at 0.7 ML, we observe another surface domain transition: both the facet and the terrace remain unchanged in their size (width), i.e., the periodicity of the surface pattern is preserved [see Fig. 2(g) vs Fig. 2(e)]; yet the (5×2) terraces convert to $(\sqrt{3}\times\sqrt{3})$ terraces [Fig. 2(h)], identical to what is observed on a nominally flat Si(111) surface at Au coverages above 0.8 ML,[3–5] whereas the facet structure remains unchanged, as shown in Fig. 2(g). Since the $(\sqrt{3}\times\sqrt{3})$ superstructure has a much higher Au coverage than the (5×2) has, we can conclude that at this step the Au atoms have self-selected to predominantly adsorb onto the terrace domains.

Combining all the results in Fig. 2, we find a very interesting self-selective Au adsorption sequence onto the self-organized Si(111) surface patterns. As the Au coverage increases, Au atoms adsorb alternatively on the facet or terrace domains, first onto the facets at 0.07 ML [Fig. 1(a)], then to the terraces at 0.3 ML [Fig. 1(c)], back to the facets at 0.5 ML [Fig. 1(e)], and then again to the terraces at 0.7 ML [Fig. 1(g)]. At each stage, Au induces a structural transformation in the Au-adsorbed facets or terraces, so as to change the relative chemical reactivity of the facet versus terrace with further deposition of Au, leading to complex evolution of surface morphologies. Despite the complexity, however, all the surface morphologies and their evolution can be understood within one unified theoretical framework, i.e., the model of elastic surface stress domains.[10,12–14]

The first intriguing observation is the constant periodicity independent of Au coverage. It indicates that as Au atoms selectively adsorb onto either facets or terraces to change the facet or terrace structure and hence their relative population, all the changes are local that the transport of Au and Si atoms are confined to two neighboring facet and terrace domains. Consequently, only the relative population of the two domains within a period changes but the periodicity remains intact. More interestingly, this constant periodicity is a universal length scale, originated by energy minimization of stress domains during the quenching of vicinal Si(111) surface,[10] which is independent of surface miscut angle. Especially we found it is preserved on all miscut surfaces upon Au deposition, as shown in Fig. 4.

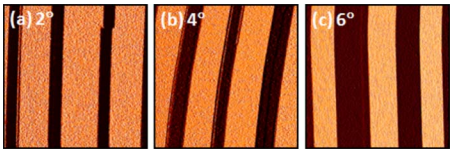

FIG. 4. (Color online) Comparison of surface morphologies of different miscut surfaces, showing the same periodicity and identical facet (1.6 nm terraces) and terrace (5×2) structures at Au coverage of 0.5 ML. Slight curvature in facets is caused by a drift of the tip during scan. Image size: 180×180 nm^2.

Second, given the constant periodicity, the relative domain population within each period is uniquely defined by the facet and miscut angle, i.e., $l_t/l_f=\tan\theta_f/\tan\theta-1$ because only certain low-energy facets with well-defined facet angles can appear, leading to well-ordered domain patterns at specific Au coverages as shown in Fig. 2. At other coverages the surfaces appear disordered. Assuming these faceted domains are local energy minimum, it is straightforward to show the optimal domain width also satisfies the condition

$$\frac{l_f}{L}=\frac{1}{\pi}\cot^{-1}\frac{\alpha}{\pi},\quad \alpha=\frac{L^2(F_f\sec\theta-F_t)}{c}. \tag{2}$$

Here α represents the ratio of the change in surface energy to the elastic relaxation energy (related to the change in surface stress) associated with the change in domain structure. In other words, when the low-energy domain (either facet or terrace) grows at the expense of the high-energy domain upon selective Au adsorption, there is an associated extra energy cost in elastic energy. From the measured domain populations, we can estimate the constant α for different Au coverages, as shown in Table I, which allow us to analyze the evolution of terrace/facet surface energies upon Au adsorption.

$\alpha=0$ means the equal domain population and the energies of terrace and facet are degenerate. For clean surface, $\alpha>0$, indicating the surface energy of the (7×7) terrace (majority domain) is lower than that of facet (minority domain). At 0.07 ML, α adopts a large negative value, indicating the energy of facet (growing to be the majority domain) has become much lower than that of terrace (shrinking to be the minority domain). This is likely because all the Au atoms have adsorbed onto the facet, decorating the steps and saturating the dangling bonds to lower its energy. At 0.3 ML, α changes to have a smaller negative value, indicating that the energy difference between facet and terrace becomes smaller

TABLE I. The values of α at different Au coverages.

Coverage (ML)	l_f (nm)	θ (deg)	α
0.0	31	12.7	0.23
0.07	55	7.2	−6.0
0.3	48	8	−2.92
0.5	35	11	−0.38
0.7	35	11	−0.38

than that at 0.07 ML and/or the surface stress discontinuity at the domain boundary becomes larger. This is possibly due to the Au adsorption onto terrace converting it into a low-energy (5×2) superstructure. The same α values at the 0.5 ML and 0.7 ML Au coverage indicate that the relative stability of the facet and terrace is about the same in these two cases.

Our findings of Au-induced structural transformation in the self-organized vicinal Si(111) surface patterns, as shown in Fig. 2, provide a unique method for the controlled surface functionalization. Because surface reactivity is expected to depend sensitively on the surface structure, such as facets with high step density vs flat terraces, and on the Au coverage, one should be able to tune the overall surface reactivity as well as the relative reactivity between individual domains simply by changing Au coverage in a very systematic way. To demonstrate this possibility, we have further deposited Co atoms onto the Au-functionalized vicinal Si(111) surfaces as a way to direct the self-assembly of $CoSi_2$ nanoclusters.

Surface patterns have been effectively used as templates to direct self-assembly of quantum dots to improve their spatial and size uniformity.[16] It has been reported that when Co atoms are deposited on a clean vicinal Si(111) surface, $CoSi_2$ nanoclusters are exclusively formed in the facet domains, leaving the terraces completely empty.[17] This is presumably because the facet consisting of bunched steps has a high density of dangling bonds giving rise to a high reactivity. However, we have achieved in directing the $CoSi_2$ nanoclusters to form exclusively in the flat terraces in the Au-functionalized vicinal Si(111) surfaces. By depositing Co atoms onto a Au-functionalized 4° Si(111) vicinal surface where terraces and facets show the (5×2) superstructure and 1.6-nm-wide mini terraces, respectively, similar to what is shown in Figs. 2(e) and 2(f), we are able to grow $CoSi_2$ nanoclusters on the terraces only, as shown in Fig. 3(b). Figure 3(c) shows the corresponding histogram of $CoSi_2$ nanocluster size distribution, which exhibits a good size uniformity with an average size of 7.1 nm. The size uniformity is possibly due to the stabilization effect induced by surface stress and bulk strain in the nanoclusters.[18]

In conclusion, we have demonstrated a self-selective surface functionalization process via Au adsorption on self-organized vicinal Si(111) surface domain patterns. At the different stage of Au deposition, Au atoms self-select to adsorb alternately onto the facet or terrace domains, and transform the domain structures and hence relative reactivity of the two domains in the surface. This leads to a complex evolution of surface pattern morphology, with the relative domain population varying with the Au coverage while the periodicity of the surface pattern being preserved, which can be understood with a stress-domain model. Furthermore, the Au-functionalized surfaces are used as nanoscale templates to direct the self-assembly of $CoSi_2$ nanoclusters. Our approach might be generalized to functionalize other surfaces of stress-domain patterns for the directed self-assembly of surface-based nanostructures.

We thank C. H. Wu, C. S. Huang, S. A. Cheng, Y. Z. Du, and B. H. Chen for carrying out parts of the adsorption experiment. F.K.M. thanks support provided by NSC of Taiwan, ROC. F.L. thanks support from NSF (Grant No. DMR-0909212) and DOE-BES (Grant No. DE-FG02-04E46148).

*phymen@ccu.edu.tw

[1] A. A. Baski, J. Nogami, and C. F. Quate, Phys. Rev. B **41**, 10247 (1990).
[2] W. Świëch *et al.*, Surf. Sci. **253**, 283 (1991).
[3] J. Nogami, A. A. Baski, and C. F. Quate, Phys. Rev. Lett. **65**, 1611 (1990).
[4] I. H. Hong, D. K. Liao, Y. C. Chou, C. M. Wei, and S. Y. Tong, Phys. Rev. B **54**, 4762 (1996).
[5] H. M. Zhang, T. Balasubramanian, and R. I. G. Uhrberg, Phys. Rev. B **65**, 035314 (2001).
[6] M. Jałochowski *et al.*, Surf. Sci. **375**, 203 (1997).
[7] M. Horn-von Hoegen *et al.*, Surf. Sci. **433-435**, 475 (1999).
[8] R. J. Phaneuf, N. C. Bartelt, E. D. Williams, W. Swiech, and E. Bauer, Phys. Rev. Lett. **67**, 2986 (1991).
[9] R. J. Phaneuf, N. C. Bartelt, E. D. Williams, W. Swiech, and E. Bauer, Phys. Rev. Lett. **71**, 2284 (1993).
[10] F. K. Men, F. Liu, P. J. Wang, C. H. Chen, D. L. Cheng, J. L. Lin, and F. J. Himpsel, Phys. Rev. Lett. **88**, 096105 (2002).
[11] K. Takayanagi *et al.*, J. Vac. Sci. Technol. A **3**, 1502 (1985).
[12] V. I. Marchenko, JETP Lett. **33**, 381 (1981).
[13] O. L. Alerhand, D. Vanderbilt, R. D. Meade, and J. D. Joannopoulos, Phys. Rev. Lett. **61**, 1973 (1988).
[14] A. Li, F. Liu, D. Y. Petrovykh, J. L. Lin, J. Viernow, F. J. Himpsel, and M. G. Lagally, Phys. Rev. Lett. **85**, 5380 (2000).
[15] S. C. Erwin, I. Barke, and F. J. Himpsel, Phys. Rev. B **80**, 155409 (2009).
[16] H. Hu, H. J Gao, and F. Liu, Phys. Rev. Lett. **101**, 216102 (2008), and references therein.
[17] I. Goldfarb, Nanotechnology **18**, 335304 (2007).
[18] F. Liu, Phys. Rev. Lett. **89**, 246105 (2002).